Supplementary Data

Confirmation of the design of the polydimethylsiloxane (PDMS) stamp

To check the design of the new PDMS stamp, we stamped fluorescent molecules and confirmed the stamped pattern following the protocol developed for the DNA garden method (1). A coverslip (Matsunami Glass Ind. Ltd.) was immersed in the solution containing 10% NH_3 and 10% H_2O_2 for a 20 min wash. After the wash, 100 μL of 0.5% MPC polymer (Lipidure-CM5206; NOF Corp., Tokyo, Japan) in 99.5% ethanol was dropped onto the coverslip and dried to coat the surface with the polymer to prevent the adsorption of DNA and p53. Next, 20 μL of a solution containing 40 nM Q-dot (Qdot 655 streptavidin conjugate, Thermo Fisher Scientific) or 77 μg/mL Alexa635-streptavidin (Thermo Fisher Scientific) in 10 mM phosphate buffer at pH 7.4 was dropped onto the PDMS stamp and was incubated for 45 min. The stamp was washed thrice with 1 mL of ultrapure water. To transfer Q-dot or Alexa635-streptavidin from the stamp to the coverslip, the coated coverslip was set on the stamp on which 300 g of weight was applied for 5 min. After stamping, the flow cell with a linear flow path was constructed using the coverslip, the slide glass with two holes, and a double-sided tape whose thickness was 100 μm. A buffer solution containing 10 mM phosphate at pH 7.4 and 2

mM Trolox was introduced into the cell and the fluorescence image of the stamped area was observed using a total internal reflection fluorescence microscope (Figure S1c-f).

Validation of the pseudo-first-order approximation for the analysis of the stopped-flow data

To achieve the pseudo-first-order process, the competitor DNA has to be excess compared to the 6-FAM DNA-p53 complex. In the current stopped-flow measurements, the prepared concentrations of the 6-FAM DNA, the p53 tetramer and the competitor DNA were 20, 30, and 50-200 nM, respectively, after the mixing in the stopped-flow device. We used the concentration of p53 slightly higher than that of 6-FAM DNA due to an unavoidable adsorption of p53 to the surface of the stopped flow reservoir and flow channels. We roughly estimate that the adsorption reduces the actual concentration of p53 to less than 20 nM, since we could not detect any anisotropy change when we conduct the experiment at 10-nM p53. Accordingly, the concentrations of the complex between 6-FAM DNA and p53 immediately after the stopped-flow mixing might be smaller than 20 nM. However, if we assume the maximum concentration of the complex between 6-FAM DNA and p53, the lowest concentration of the competitor DNA (50 nM) was only 2.5-fold higher than that of the complex, suggesting that the pseudo-first-order

approximation might not be valid. In contrast, at the concentration range of the competitor more than 100 nM, the competitor concentration was at least more than 5 times larger than that of the complex. Thus, the pseudo-first-order approximation should be valid at the concentration range of the competitor DNA more than 100 nM.

To further examine the validity of the pseudo-first-order approximation, we plotted the fitting residuals of the time courses of the anisotropy values in Figure 2b from the single-exponential curve (Figure S2). If the pseudo-first-order approximation was not satisfied, the concentration of the competitor at the later end of the time course becomes significantly smaller, causing a slower decrease of the anisotropy values at the later time end compared to the single exponential curve. However, even for the lowest competitor concentration of 50 nM, the residuals were centered around 0 and showed no systematic time dependent changes, supporting the validity of the single exponential fitting. The results suggested that the actual concentration of the complex might be less than 20 nM.

Given the above considerations, we fitted the time courses of the anisotropy values obtained at all the competitor concentrations with the single-exponential function. However, since the k_{obs} values obtained at 50-nM competitor DNA might not be reliable, the kinetic rate constants obtained at this condition were used only as reference. We determined the rates of IST (k_{IST}) by fitting the plots of the apparent dissociation rate

constants obtained at 100-200 nM of the competitor DNA with a linear function.

The transfer efficiency (TE) should be affected by the variation of the distance between the two DNA strands

The TE values obtained in the single-molecule measurements should be affected by the variation of the distance between two DNA strands, since two DNAs have to be close to each other during IST. The fluctuation of the tethered DNA provides the variation of the distance between two DNA strands. In addition, the width of the stamped lattices (2 or 3 μm) might cause the variation in the tautness of the tethered DNA strands, affecting their fluctuation. Because the movement of p53 along DNA could be tracked by the TIRF microscopy, the fluctuation of the DNA strands should occur within the evanescent field, which is ~200 nm in height. Accordingly, the distance variation between two DNA strands, estimated within ~200 nm, can cause the uncertainty of the obtained TE values.

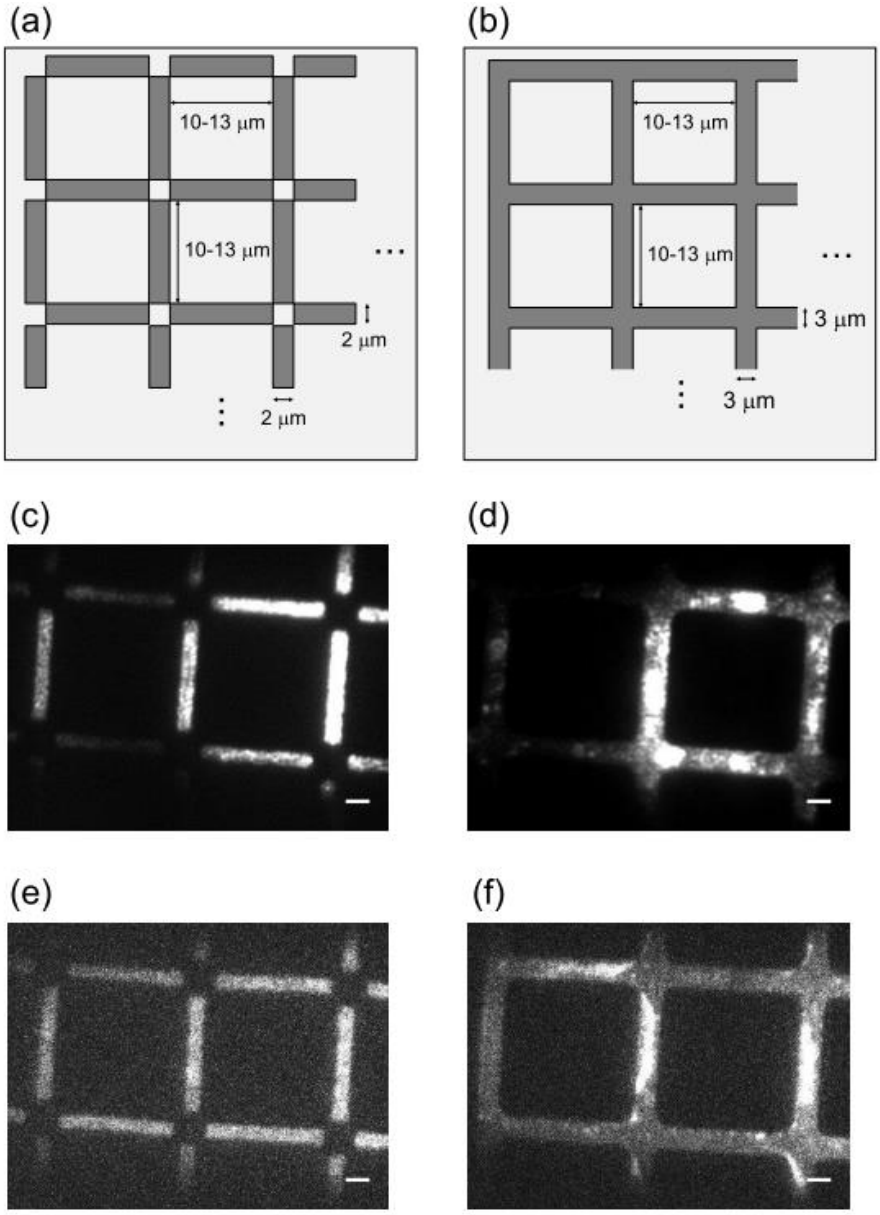

Figure S1. Design of the PDMS stamp prepared for construction of crisscrossed DNA strands. (a, b) Patterns of the designed PDMS stamp. Dark gray areas denote the regions for stamping. The widths of the gray area are 2 μm (a) and 3 μm (b). Four types of lattices were prepared for each pattern, with 10, 11, 12, and 13 μm of distance between the two parallel lines. (c-f) Fluorescence images of the stamped Q-dots (c and d) and

Alexa635-streptavidin (e and f). Typical images obtained for the coverslip stamped with 40 nM of Q-dot and 77 μg/mL of Alexa635-streptavidin are presented. Scale bars represent 2 μm.

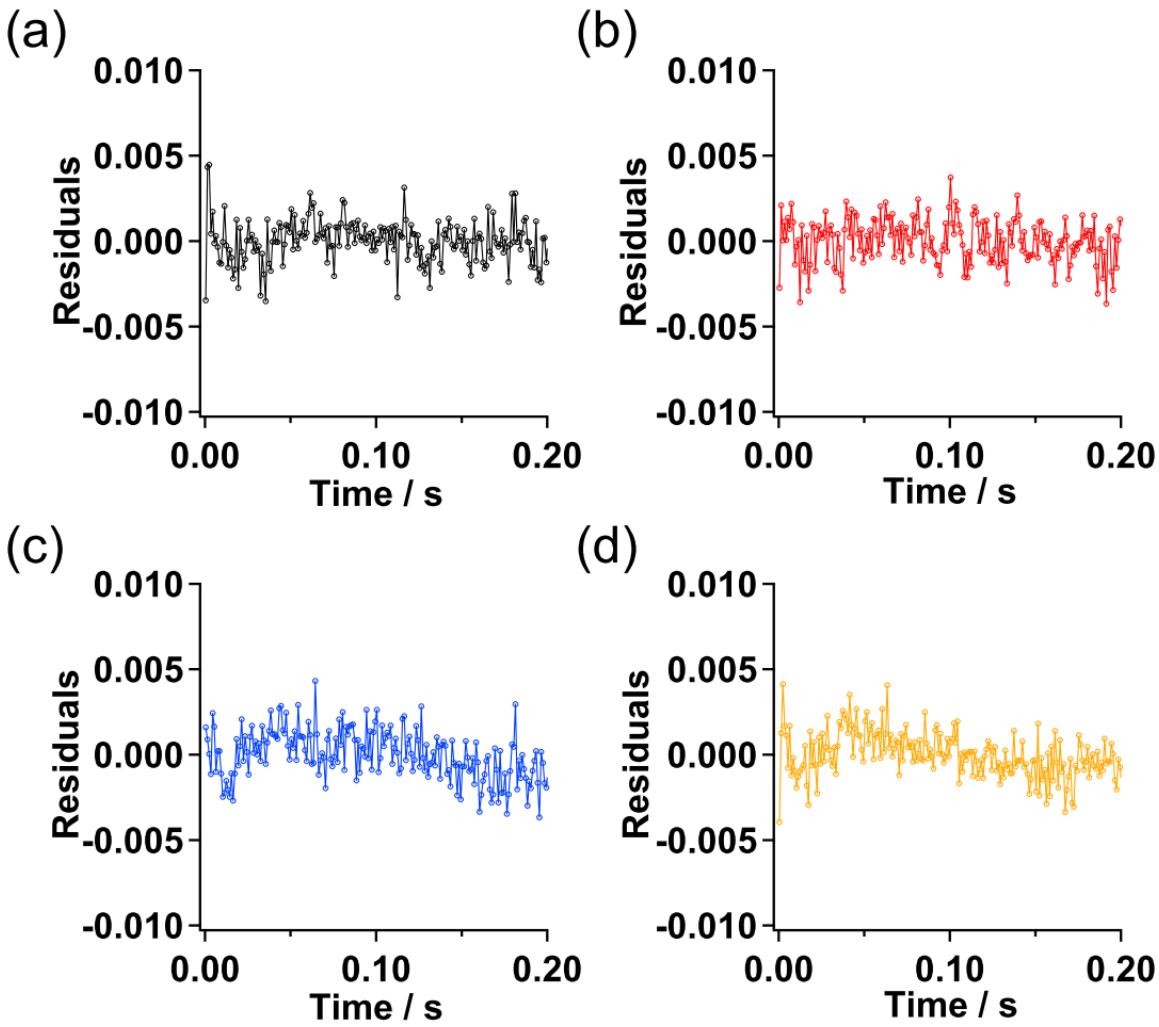

Figure S2. The fitting residuals of the kinetic anisotropy values by the single-exponential curve. The time dependent anisotropy values of the 6-FAM labeled non-target DNA bound to p53 after the stopped flow mixing with various concentrations of the competitor DNA were obtained (Figure 2b). The data were fitted with the single-exponential function and the residuals of the fitting were presented. The time courses were obtained after mixing (a) 50, (b) 100, (c) 150, and (d) 200 nM of the competitor DNA.

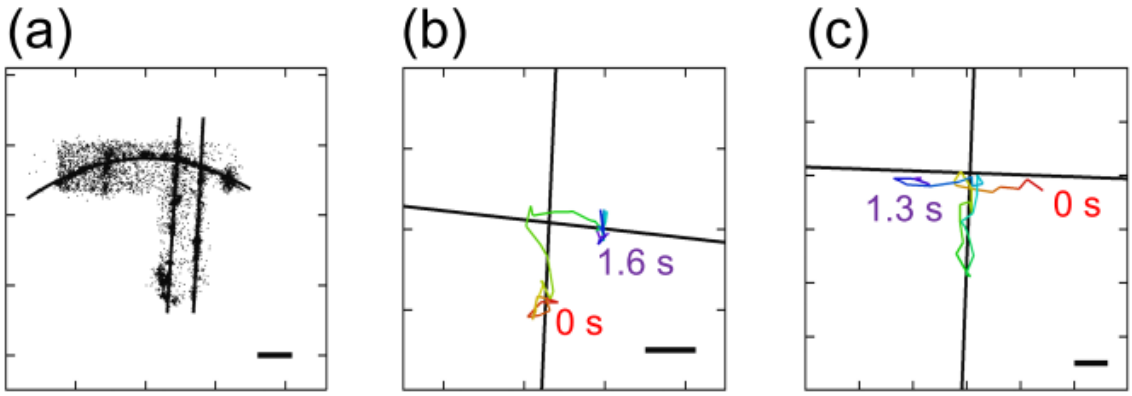

Figure S3. (a) Determination of the position of the tethered DNA strands and their intersections. The image corresponds to the same area shown in Figure 5b in the main text. The black dots correspond to all the tracked coordinates of ATTO532-pseudo-WT p53 plotted in one image. Two vertical lines and one curved line correspond to the positions of DNA strands obtained by fitting the coordinates of p53 with a linear (vertical) and quadratic (horizontal) function. To simplify the figure, we only showed the coordinates of p53 located in the vicinity of DNA strands forming the intersection. Scale bar in panel (a): 2 μm. Representative trajectories depicting IST of (b) pseudo-WT and (c) TetCT in the presence of 25 mM K^+ and 2 mM Mg^{2+}. Black solid lines and rainbow curves denote DNA and the time course of the trajectories in which red is the starting point, 0 s, respectively. Scale bars in panels (b) and (c): 0.5 μm.

Table S1. IST rates of the p53 mutants (k_{IST})

p53	6-FAM DNA	$[K^+]$ / mM	$[Mg^{2+}]$ / mM	k_{IST} / 10^8 M^{-1} s^{-1}	Figure
Pseudo-WT	Target	50	2	No IST	2c
Pseudo-WT	Non-target	50	2	3.6 ± 0.3	2c, 4a, 4c
Inactive	Target	50	2	2.1 ± 0.5	2d
Inactive	Non-target	50	2	2.0 ± 0.3	2d
Pseudo-WT	Non-target	50	1	2.5 ± 0.2	3b, 4c
TetCT	Non-target	50	1	4.7 ± 0.8	3b
CoreTet	Non-target	50	1	No IST	3b
Pseudo-WT	Non-target	0	2	1.5 ± 0.1	4a
Pseudo-WT	Non-target	100	2	8.7 ± 0.8	4a
Pseudo-WT	Non-target	50	0	0.4 ± 0.1	4c
Pseudo-WT	Non-target	50	3	3.6 ± 0.4	4c

Errors are fitting errors.

Table S2. The number of events for the movement of p53 near the intersection of two DNA strands observed by single-molecule fluorescence measurements

p53	$[Mg^{2+}]$ / mM	$N_{Transfer}$	N_{Pass}	N_{Return}	$N_{Dissociation}$	TE / %
Pseudo-WT	0	10 ± 3	3 ± 2	24 ± 4	22 ± 4	17 ± 5
TetCT	0	24 ± 5	5 ± 2	65 ± 6	68 ± 6	15 ± 3
CoreTet	0	0	1 ± 1	11 ± 2	8 ± 2	0
Pseudo-WT	2	4 ± 2	1 ± 1	26 ± 3	13 ± 3	9 ± 4
TetCT	2	31 ± 5	11 ± 3	51 ± 5	27 ± 5	26 ± 4

Errors were calculated by the bootstrap method with 1000 replicates (2). TE stands for transfer efficiency.

References

1. Igarashi, C., Murata, A., Itoh, Y., Subekti, D.R.G., Takahashi, S. and Kamagata, K. (2017) DNA garden: a simple method for producing arrays of stretchable DNA for single-molecule fluorescence imaging of DNA binding proteins. *Bull. Chem. Soc. Jpn.*, **90**, 34-43.

2. Efron, B. and Tibshirani, R.J. (1993) *An Introduction to the Bootstrap* Chapman and Hall/CRC